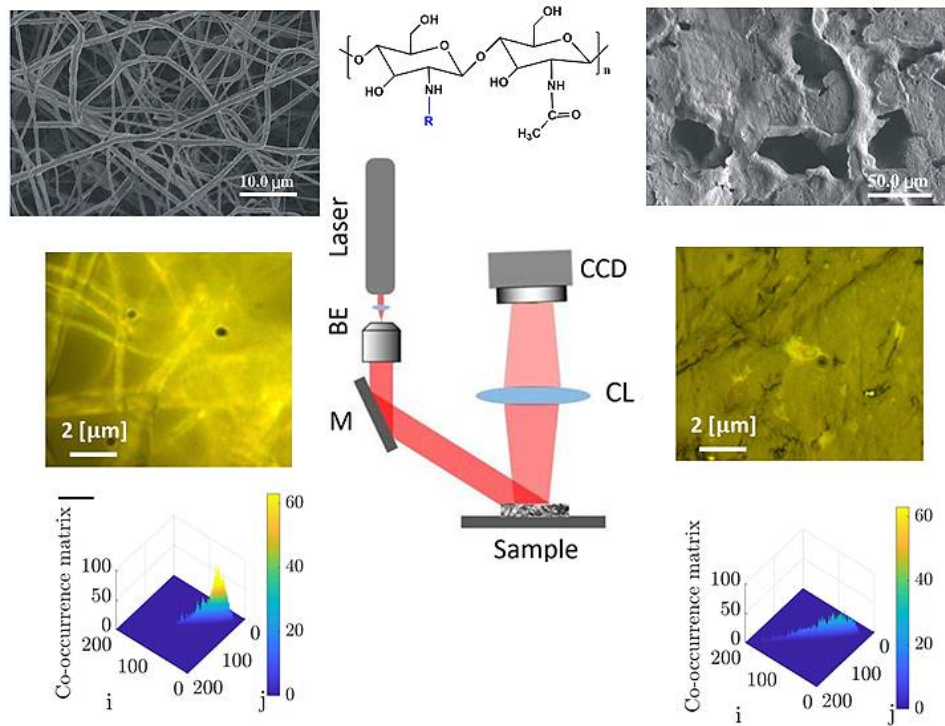


Graphical Abstract



Surface characterizations of membranes and electrospun chitosan derivatives by optical speckle analysis

Muhammad Rizwan^{a,b}, Yasaman Ganjkhani^c, Vahideh Farzam Rad^c, Maasoomeh Bazzar^d, Muhammad Yar^{e,*}, Rosiyah Yahya^a, Ali-Reza Moradi^{c,f,*}

^aDepartment of chemistry, Universiti Malaya, Kuala Lumpur, 50603, Malaysia;
rizi_chem1981@hotmail.com (M.R), rosiyah@um.edu.my (R.Y)

^bDepartment of chemistry, The University of Lahore, Lahore, Pakistan.

^c Department of Physics, Institute for Advanced Studies in Basic Sciences (IASBS), 45137-66731, Zanjan , Iran; ganjkhaniyy@iasbs.ac.ir, y.farzamrad@iasbs.ac.ir, moradika@iasbs.ac.ir

^d School of Chemistry, University of East Anglia, Norwich Research Park, Norwich NR4 7TJ; m.bazzar@uea.ac.uk

^e Interdisciplinary Research Center in Biomedical Materials, COMSATS University, 54000, Lahore, Pakistan; drmyar@cuilahore.edu.pk (M.Y)

^f School of Nano Science, Institute for Research in Fundamental Sciences (IPM), 19395-5531, Tehran, Iran.

Correspondence:

*Ali-Reza Moradi; Department of Physics, Institute for Advanced Studies in Basic Sciences (IASBS), 45137-66731, Zanjan, Iran; moradika@iasbs.ac.ir

*Muhammad Yar; Interdisciplinary Research Center in Biomedical Materials, COMSATS University, 54000, Lahore, Pakistan; drmyar@cuilahore.edu.pk

Abstract

In this paper we show that laser speckle pattern provides useful information toward revealing discrimination between nanofibers and membranes. Chitosan materials particularly organo-soluble chitosan derivatives have a number of applications. The surface characteristics of these materials are very critical for specific applications. The analysis of laser speckles, both numerical and

graphical, includes information about the surface structure. The development of digital electronics brought the ease of image processing and has opened new perspectives for a spectrum of laser speckle analysis (LASCA) applications. Our results show reasonable differences between the LASCA parameters of nanofibers and membranes. The methodology may be considered as a quantitative assessment tool for similar samples.

Keywords: Chitosan derivatives; Membranes; Electrospun nanofibers; Laser Speckle Analysis

Introduction

The visualization of surface structure is of fundamental importance for a wide variety of biological and biomedical applications, such as obstruction, stiffness, and response to an external stimulus. Laser speckle analysis (LASCA) is a nondestructive and non-contact technique for that task which is based on the spatio-temporal integration of the scattered light from a sample when illuminated by a coherent light [1-3]. This technique is single shot, suitable for characterizing both solid and liquid samples, non-contact and non-destructive with a large field of view, and doesn't need any specific preparation of the sample. Other surface characterization techniques such as SEM and AFM can be applied to such surfaces, but they have their own limitations. SEM for example, although being high resolution and suitable for 3D imaging, is expensive, large and must be housed in an area free of any possible electric, magnetic or vibration interference. Sample preparation is required, which can result in artifacts and errors and might be damaging to samples. In addition, SEMs are limited to solid, inorganic samples small enough to fit inside the vacuum chamber that can handle moderate vacuum pressure. There is also a small risk of radiation exposure, which needs careful attention to safety precautions. AFM, in comparison to SEM, is free of special sample treatment, expensive vacuum environment and high maintenance and can be higher in resolution and used for liquids also. However, its scanning speed is slow, can be destructive due to the tip

contacting the sample and is unable to work for dynamic specimens and for steep valleys and peaks [4-8]. LASCA has been applied in the fields of medicine, e.g. blood flow through veins in the skin surface and in internal organs, agriculture, e.g. evaluation of quality of crops and to monitor beef aging [9, 10], microfluidics, e.g. optical scattering variation in biological fluids [11] and determining particle viscoelastic properties through laser speckle rheology [12, 13], and microbiology e.g. monitoring the variations of bacteria and parasites [14, 15].

In LASCA, speckle patterns are formed due to the interference of the light scattered from the fluctuations of the reflective samples or thickness variations of the transparent samples [16, 17]. When a coherent beam of light is scattered from a rough surface, the scattered light from each point of the surface reaches into each pixel of the detector. Therefore, every point on the detector includes some information of the sample. The speckle pattern derived in this way has a particular texture and by analyzing these textures, the information related to the samples is extracted.

Chitosan (CS) is obtained by the deacetylation of chitin, second most abundant natural polymer. It is selected in this work as a base material owing to its non-toxicity, biodegradability and biocompatibility. The CS chains consists of repeat units, *N*acetyl*D*glucosamine and *D*glucosamine which are linked through 1,4glycosidic linkages. The former unit decides the degree of deacetylation CS [18]. Poor solubility of CS in water at pH higher than 6.0 and insolubility in organic solvents limits its applications in biomedical fields [19]. The rigid crystalline structure of CS is mainly responsible for the insolubility which is attributed to strong inter- and intramolecular hydrogen bonding in the structure. The introduction of hydrophobic moieties at -NH₂ and/or -OH groups [20] makes CS soluble in organic solvents to design novel functional biomaterials.

CS is vulnerable to different types of chemical modifications such as alkylation [21], carboxymethylation [22], graft copolymerization [23], benzoylation [24] and sulphation [25]

owing to the presence of reactive groups ($-\text{NH}_2$ at C-2 > $-\text{OH}$ at C-6) along its chains. Comprehensive reports are available on water soluble chitosan derivatives [26] in the recent literature which are mostly pH sensitive [27-29] whereas few reports are available on organosoluble chitosan derivatives. Ma *et al.* synthesized organosoluble acetylated CS by the reaction of stearoyl chloride and CS [30]. Ping Zhang and Moyuan Cao synthesized a novel organosoluble glycidyl grafted CS [31] while Renbutsu *et al.* synthesized organosoluble CS derivatives from the natural sources for UV curable products and for biomedical applications [32]. Organosolubility of CS derivatives made it possible to be blended with some other commercial biocompatible polymers which helps in developing a material with properties additive of the two polymers.

PCL is a biocompatible, biodegradable with low degradation rate and elastic biomaterial with high elongation break [33]. Owing to its slow degradation and drug permeability, it is a leading candidate for long term implants and drug delivery applications. Being hydrophobic, PCL is soluble in a variety of organic solvents and can be blended with other organosoluble polymers e.g. polylactic acid and polylactic acid-co-glycolic acid to manipulate the drug release rate and to address required tissue engineering characteristics [34]. PCL, due to its good mechanical stability and hydrophobic nature is used as a base material for the tissue engineering.

Blends of Chitosan with some other natural and synthetic polymers have been reported to get nanofibrous membranes with enhanced properties such as (i) chitosan/gelatin blended nanofibers [35] and polyelectrolyte complex [36] with enhanced antibacterial and mechanical properties (ii) different chitosan blends in anti-inflammatory and wound healing applications [37] (iii) photocrosslinked chitosan/poly(vinyl alcohol) blends with varying capacity of water resistance owing to cross-linking density [38] (iv) various chitosan blended membranes have been used for adsorptive purpose from waste water from industries containing dyes and heavy metals

as impurities [39]. Previously, our group have reported chitosan derivatives with enhanced organosolubility, antibacterial activity and controlled biodegradation and their composite with PCL as nanofibrous mate and membranes exhibiting enhanced angiogenesis in *ex-ovo* CAM assay [40, 41]. In this paper, by exploring a representation based on the homogeneity values and cooccurrence matrix of the associated speckle patterns, it is possible to characterize and examine the chitosanbased samples. Moreover, a relationship between the surface structure and the aforementioned parameters is demonstrated in current study.

Materials and methods

All the materials and methods has been reported in our papers [40, 41] and is given as supplementary materials.

Results and discussions

Synthesis of chitosan derivatives

In our previously published papers [40, 41] the two CS derivatives, CSD-I and CSD-II were synthesized by the reaction of CS with 1,3DETBA and 1,3-DMBA, respectively in separate containers in the presence of TEOF as linker (Figure 1). The reaction was carried out in solvent mixture of acetic acid:methanol (1:4) at 70 °C.

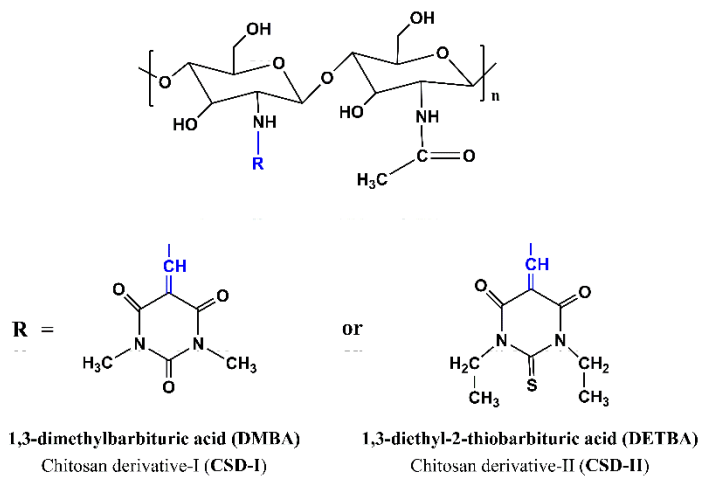


Figure 1: Chemical structure of CS derivatives, CSD-I and CSD-II.

Membrane formation and electrospinning of blended solutions of CS derivatives with PCL

The improved solubility of CS derivatives, CSD-I and CSD-II made it possible to be blended with PCL, a multipurpose synthetic, biocompatible, FDA approved material in biomedical field [42-44] to form a homogeneous solution in organic solvents; chloroform, DMSO and DMF. The blended solution of each derivative was divided into two parts; one part was used to prepare films and other part was used to prepare nanofibers by electrospinning. The samples were designated as CSD-I-M (membrane), CSD-I-NF (nanofibers) and CSD-II-M (membrane), and CSDIIINF (fibers) prepared from CSD-I/PCL and CSDII/PCL blends, respectively.

The morphologies of CSD-I/PCL and CSD-II/PCL films were studied using FESEM which showed porous sponge-like structure of membrane (Figure 2); micropores in the structure were observed.

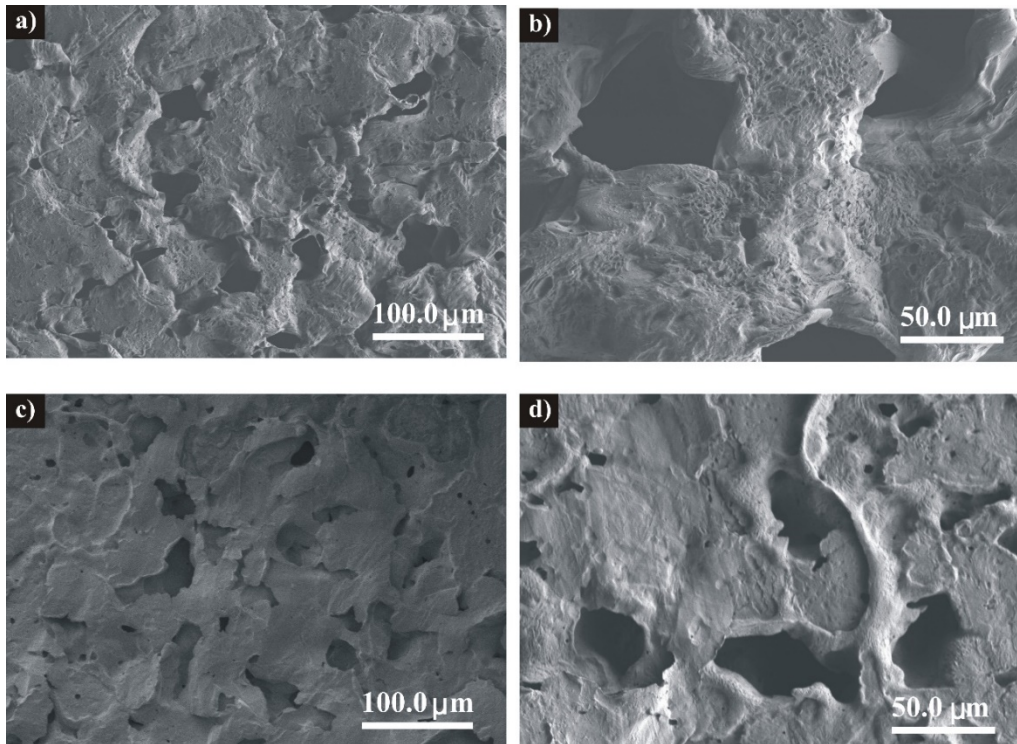


Figure 2: FESEM images of a,b) CSD-I/PCL c,d) CSD-II/PCL blended membrane.

The FESEM images of electrospun nanofibers revealed that the fibres were beads free with random orientation and an average diameter of 360 nm (Figure 3a,b,c) for CSD-I/PCL and 540 nm (Figure 3d,e,f) for CSD-II/PCL. The fibre surface was observed to have their smooth surface which undoubtedly reflects the uniform and homogeneous mixing of CSD-I and CSD-II with PCL in organic solvents [45, 46]. From the results, we deduce that it is possible to blend CSD-I and CSD-II with PCL at different ratios to obtain beads free fibers as long as the right combination of co-solvents are used.

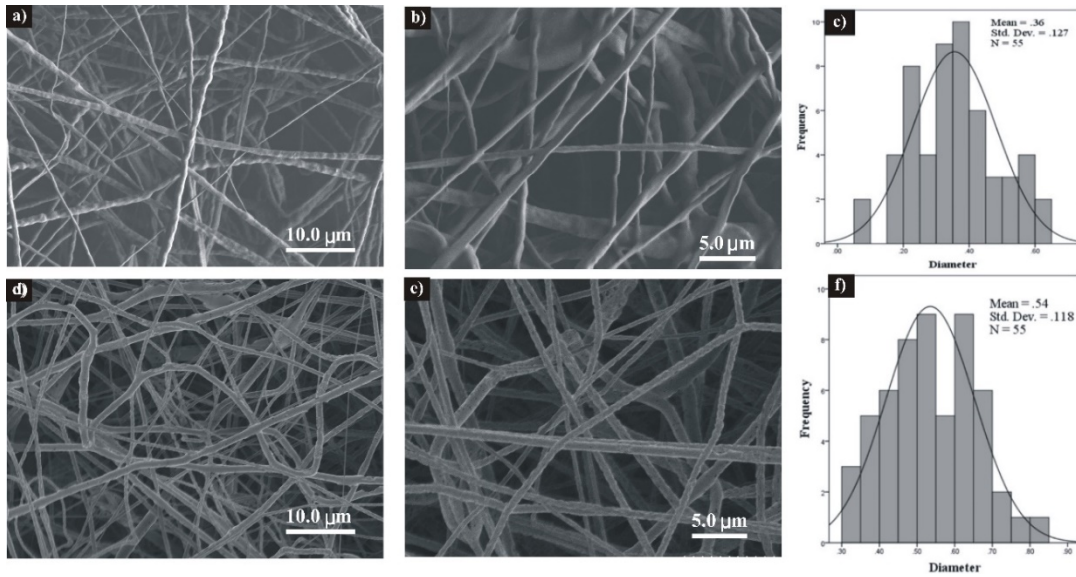


Figure 3: FESEM images of electrospun nanofibers along with their histograms showing fiber diameter distribution; a,b,c) electrospinning of solution CSD-I/PCL blended solution and d,e,f) electrospinning of CSD-II/PCL blended solution.

Laser speckle analysis

Figures 4 (a-d), show the conventional reflective microscopy (Nikon, Eclipse 50i Pol) images of CSD-I-M, CSD-I-NF, CSD-II-M, and CSD-II-NF, respectively, taken using a 100× objective (Dry, NA=0.8).

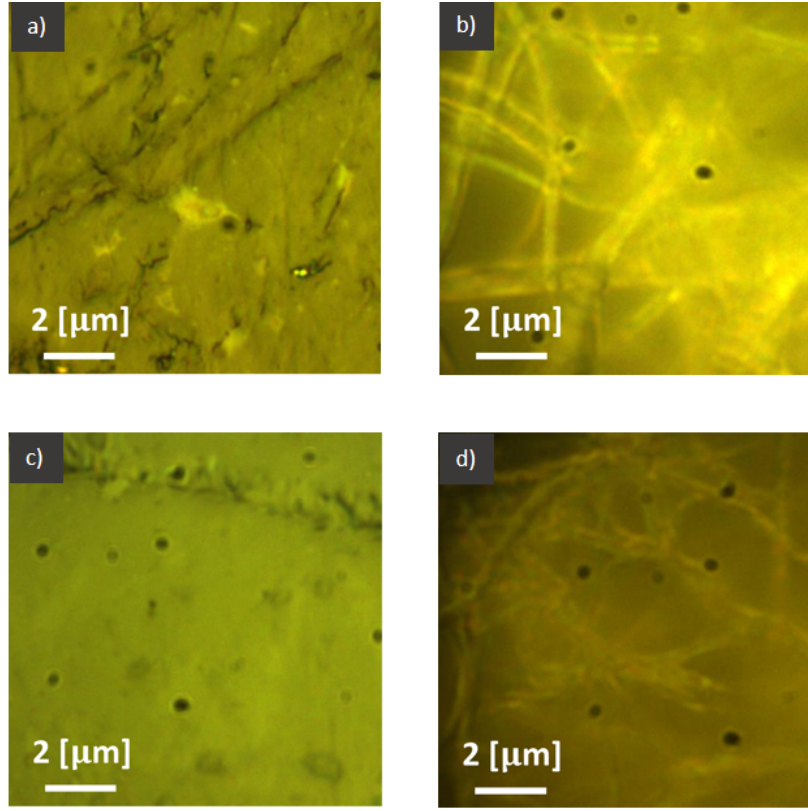


Figure 4: Microscopy images of a) CSD-I-M, b) CSD-I-NF, c) CSD-II-M, and d) CSD-II-NF.

The scheme of the setup is shown in Fig. 5 (a). The collimated laser beam (Diameter=5cm, He-Ne, 632.8 nm) illuminates the samples, and the scattered beam from the sample is collected by the collecting lens (CL) and is imaged onto the camera (DCC1545M, Thorlabs, 8-bit dynamic range, 5.2 μm pixel pitch). The CL and the camera are placed at 11 cm and 28 cm above the sample, respectively. For analysing the speckle pattern, a number of patterns are needed to be recorded successively as a data pack. A sample speckle pattern of the CSD-I-M is shown in Fig. 5(b).

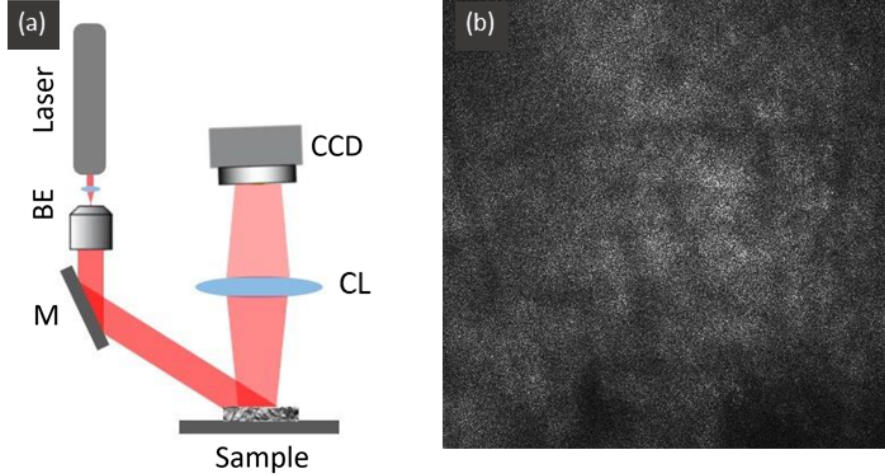


Figure 5: a) Schematic configuration of the LASCA experiments; BE: beam expander, M: Mirror, CL: lens; b) speckle pattern of the sample CSD-I-M.

The temporal history of the speckle pattern (THSP) is a matrix derived from monitoring M random pixels over N successive speckle patterns. THSP is the core of the analysis since other graphical and numerical factors related to sample structure are derivatives of this matrix. The cooccurrence matrix (COM) is a graphical representation of the distribution of intensities and is evaluated by calculating the frequency at which a pair of pixels with intensity values i and j occur in the THSP matrix:

$$\text{COM}(i,j) = \sum_{m=1}^M \sum_{n=1}^{N-1} \begin{cases} 1, & \text{if } \text{THSP}(m,n) = i \\ & \text{and } \text{THSP}(m,n+1) = j \\ 0, & \text{otherwise} \end{cases} \quad (3)$$

where, M and N are the number of points in the pattern and the number of recorded speckle patterns in the data pack, respectively. The 3D representations of the COM of the samples are shown in Figs. 6 (a-d). The distribution of the COM values around the main diagonal is a measure of roughness of the surface. The more dispersed the values, the smoother the surface structure. Moreover, the height of COM is also a measure for the roughness of the samples. As shown in

these figures, the homogeneity of the nano-fibrous CSDs is lower and they are also rougher in comparison to the membranes, whose COM matrix has more dispersion around the main diagonal.

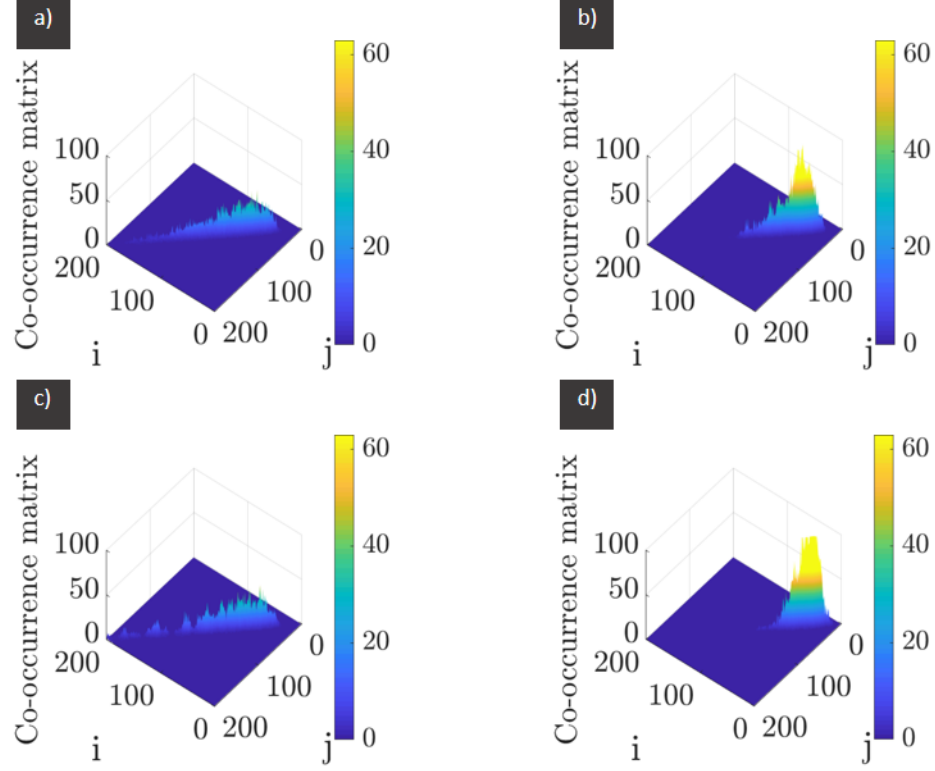


Figure 6: Co-occurrence matrix of the speckle patterns of a) CSD-I-M, b) CSD-I-NF, c) CSDIIIM, and d) CSD-II-NF.

The graphical parameter, homogeneity, is another factor to demonstrate the difference between the surfaces, which is based on the analysis of other pre-calculated parameters such as absolute value of differences (AVD):

$$AVD = \sum_i \sum_j \frac{COM(i,j)}{\sum_m COM(i,m)} |i - j| \quad (4)$$

In order to calculate the homogeneity value for each pixel, first a speckle image of $nN \times mM$ pixels is divided into windows $W(i,j)$ of $n \times m$ pixels, for all $1 \leq i \leq N$ and $1 \leq j \leq M$, the

indicator is then applied on these data and one activity indicator value $A(i,j)$ results for each window [47]. The homogeneity value H for the window $W(i,j)$ is then derived as follows:

$$H = 100 \left(1 - \frac{C_a}{C_{\max}} \right) \quad (5)$$

and,

$$C_a = \frac{\sigma_a}{\mu_a} \quad (6)$$

where, $\mu_a = \text{mean}(a)$ and $\sigma_a = \text{std}(a)$ are the mean value and the standard deviation of the set of values $a = \{A(i_0-1, j_0), A(i_0, j_0-1), A(i_0, j_0), A(i_0, j_0+1), A(i_0+1, j_0)\}$, respectively. The value C_{\max} is the maximum value of all spatial contrast values (C) in all of the windows $W(i,j)$.

In Figs. 7 (a-d) the graphical 2D demonstrations of the homogeneity of the samples are shown. The higher homogeneity values throughout the surface of membranes (Figs. 7 (a) and (c)) show the higher smoothness of these samples with respect to the nano-fibrous forms. In Fig. 7 (e), the mean values of the homogeneity parameter of the surfaces are plotted, which is in agreement with the results of the COM matrix.

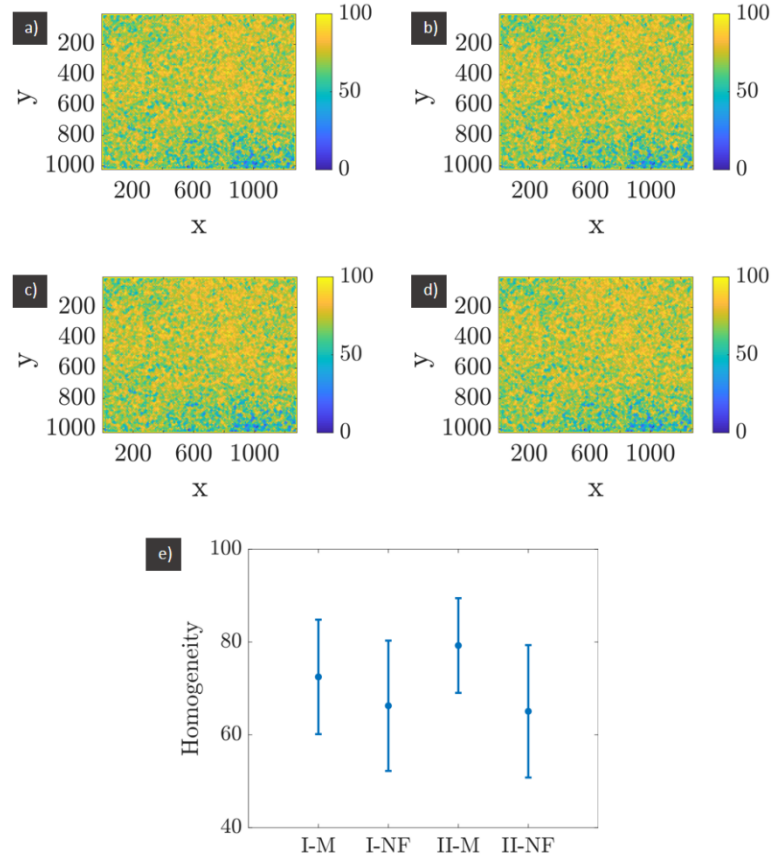


Figure 7: Surface homogeneity profiles of a) CSD-I-M, b) CSD-I-NF, c) CSD-II-M, d) CSDIINF and e) homogeneity mean values of (a-d).

Conclusion

Chitosan and chitosan organo-soluble materials are very attractive in the field of biomaterials research. Their scaffolds including membranes and fibers are very popular for producing various medical devices and wound dressings. The biological cells behave different for different surfaces, so to get the suitable surface the various analysis can be valuable. In current research, it is shown that by speckle pattern analysis as a tool for representation of the homogeneity values and the co-occurrence matrix, derived from the speckle patterns it is possible to categorize different

membranes and nanofibers. The laser speckle analysis methodology provides valuable information to characterize diffusive samples and can be applied for variety of dynamic phenomena.

Acknowledgement

M.R., M.Y. and R.Y. are indebted to the financial grants from Universiti Malaya (PG335-2016A).

References:

- [1] G.J. Richards, J.D. Briers, Laser speckle contrast analysis (LASCA): a technique for measuring capillary blood flow using the first order statistics of laser speckle patterns, IET Conference Proceedings, Institution of Engineering and Technology, 1997, pp. 11-11.
- [2] P. Miao, A. Rege, N. Li, N.V. Thakor, S. Tong, High Resolution Cerebral Blood Flow Imaging by Registered Laser Speckle Contrast Analysis, IEEE Transactions on Biomedical Engineering 57(5) (2010) 1152-1157.
- [3] V. Farzam Rad, E.E. Ramírez-Miquet, H. Cabrera, M. Habibi, A.-R. Moradi, Speckle pattern analysis of crumpled papers, Appl. Opt. 58(24) (2019) 6549-6554.
- [4] W. Zhou, R. Apkarian, Z.L. Wang, D. Joy, Fundamentals of Scanning Electron Microscopy (SEM), in: W. Zhou, Z.L. Wang (Eds.), Scanning Microscopy for Nanotechnology: Techniques and Applications, Springer New York, New York, NY, 2007, pp. 1-40.
- [5] W. Zhou, Z.L. Wang, Scanning microscopy for nanotechnology: techniques and applications, Springer science & business media2007.
- [6] L. Wilson, P.T. Matsudaira, B.P. Jena, J.K.H. Horber, Atomic Force Microscopy in Cell Biology, Elsevier Science2002.
- [7] V. Bellitto, Atomic Force Microscopy: Imaging, Measuring and Manipulating Surfaces at the Atomic Scale, IntechOpen2012.
- [8] S. Morita, F.J. Giessibl, E. Meyer, R. Wiesendanger, Noncontact Atomic Force Microscopy, Springer International Publishing2015.
- [9] R.A. Braga Jr, G.F. Rabelo, L.R. Granato, E.F. Santos, J.C. Machado, R. Arizaga, H.J. Rabal, M. Trivi, Detection of Fungi in Beans by the Laser Biospeckle Technique, Biosystems Engineering 91(4) (2005) 465-469.
- [10] I.C. Amaral, R.A. Braga, E.M. Ramos, A.L.S. Ramos, E.A.R. Roxael, Application of biospeckle laser technique for determining biological phenomena related to beef aging, Journal of Food Engineering 119(1) (2013) 135-139.
- [11] Z. Hajjarian, S.K. Nadkarni, Evaluating the Viscoelastic Properties of Tissue from Laser Speckle Fluctuations, Scientific Reports 2 (2012) 316.
- [12] Z. Hajjarian, S.K. Nadkarni, Estimation of particle size variations for laser speckle rheology of materials, Optics letters 40(5) (2015) 764-767.
- [13] Z. Hajjarian, H.T. Nia, S. Ahn, A.J. Grodzinsky, R.K. Jain, S.K. Nadkarni, Laser Speckle Rheology for evaluating the viscoelastic properties of hydrogel scaffolds, Scientific Reports 6 (2016) 37949.
- [14] H.J. Rabal, R.A. Braga Jr, Dynamic laser speckle and applications, CRC press2008.
- [15] H. Peregrina-Barreto, E. Perez-Corona, J. Rangel-Magdaleno, R. Ramos-Garcia, R. Chiu, J.C. Ramirez-San-Juan, Use of kurtosis for locating deep blood vessels in raw speckle imaging using a homogeneity representation, Journal of biomedical optics 22(6) (2017) 066004.
- [16] R. Arizaga, M. Trivi, H. Rabal, Speckle time evolution characterization by the co-occurrence matrix analysis, Optics & Laser Technology 31(2) (1999) 163-169.
- [17] R.P. Godinho, M.M. Silva, J.R. Nozela, R.A. Braga, Online biospeckle assessment without loss of definition and resolution by motion history image, Optics and Lasers in Engineering 50(3) (2012) 366-372.
- [18] M. Rizwan, R. Yahya, A. Hassan, M. Yar, A. Azzahari, V. Selvanathan, F. Sonsudin, C. Abouloula, pH sensitive hydrogels in drug delivery: brief history, properties, swelling, and release mechanism, material selection and applications, Polymers 9(4) (2017) 137.

- [19] C. Zhao-Sheng, S. Yue-Ming, Y. Chun-Sheng, Z. Xue-Mei, Preparation, characterization, and antibacterial activities of para-biguaniidinyl benzoyl chitosan hydrochloride, *Journal of Applied Polymer Science* 125(2) (2012) 1146-1151.
- [20] S. Nishimura, O. Kohgo, K. Kurita, H. Kuzuhara, Chemospecific manipulations of a rigid polysaccharide: syntheses of novel chitosan derivatives with excellent solubility in common organic solvents by regioselective chemical modifications, *Macromolecules* 24(17) (1991) 4745-4748.
- [21] F. Bertoni, N. Barbani, P. Giusti, G. Ciardelli, Transglutaminase reactivity with gelatine: perspective applications in tissue engineering, *Biotechnology Letters* 28(10) (2006) 697-702.
- [22] H. Bidgoli, A. Zamani, M.J. Taherzadeh, Effect of carboxymethylation conditions on the water-binding capacity of chitosan-based superabsorbents, *Carbohydrate Research* 345(18) (2010) 2683-2689.
- [23] G. Huacai, P. Wan, L. Dengke, Graft copolymerization of chitosan with acrylic acid under microwave irradiation and its water absorbency, *Carbohydrate Polymers* 66(3) (2006) 372-378.
- [24] D. Lee, Z.S. Quan, C. Lu, J.A. Jeong, C. Song, M.-S. Song, K.Y. Chai, Preparation and Physical Properties of Chitosan Benzoic Acid Derivatives Using a Phosphoryl Mixed Anhydride System, *Molecules* 17(2) (2012) 2231.
- [25] R. Jayakumar, N. Nwe, S. Tokura, H. Tamura, Sulfated chitin and chitosan as novel biomaterials, *International Journal of Biological Macromolecules* 40(3) (2007) 175-181.
- [26] N. Kahya, Water Soluble Chitosan Derivatives and their Biological Activities: A Review, *Polymer Science*, <https://doi.org/10.4172/2471-9935.100043>.
- [27] T. Rasheed, M. Bilal, N.Y. Abu-Thabit, H.M.N. Iqbal, 3 - The smart chemistry of stimuli-responsive polymeric carriers for target drug delivery applications, in: A.S.H. Makhlof, N.Y. Abu-Thabit (Eds.), *Stimuli Responsive Polymeric Nanocarriers for Drug Delivery Applications*, Volume 1, Woodhead Publishing2018, pp. 61-99.
- [28] H.M.N. Iqbal, T. Keshavarz, 14 - Bioinspired polymeric carriers for drug delivery applications, in: A.S.H. Makhlof, N.Y. Abu-Thabit (Eds.), *Stimuli Responsive Polymeric Nanocarriers for Drug Delivery Applications*, Volume 1, Woodhead Publishing2018, pp. 377-404.
- [29] A. Raza, U. Hayat, T. Rasheed, M. Bilal, H.M.N. Iqbal, Redox-responsive nano-carriers as tumor-targeted drug delivery systems, *European Journal of Medicinal Chemistry* 157 (2018) 705-715.
- [30] G. Ma, D. Yang, J.F. Kennedy, J. Nie, Synthesize and characterization of organic-soluble acylated chitosan, *Carbohydrate Polymers* 75(3) (2009) 390-394.
- [31] P. Zhang, M. Cao, Preparation of a novel organo-soluble chitosan grafted polycaprolactone copolymer for drug delivery, *International Journal of Biological Macromolecules* 65 (2014) 21-27.
- [32] E. Renbutsu, M. Hirose, Y. Omura, F. Nakatsubo, Y. Okamura, Y. Okamoto, H. Saimoto, Y. Shigemasa, S. Minami, Preparation and biocompatibility of novel UV-curable chitosan derivatives, *Biomacromolecules* 6(5) (2005) 2385-2388.
- [33] B.D. Ulery, L.S. Nair, C.T. Laurencin, Biomedical applications of biodegradable polymers, *Journal of Polymer Science Part B: Polymer Physics* 49(12) (2011) 832-864.
- [34] M.A. Woodruff, D.W. Hutmacher, The return of a forgotten polymer—Polycaprolactone in the 21st century, *Progress in Polymer Science* 35(10) (2010) 1217-1256.
- [35] N. Cai, C. Li, C. Han, X. Luo, L. Shen, Y. Xue, F. Yu, Tailoring mechanical and antibacterial properties of chitosan/gelatin nanofiber membranes with Fe₃O₄ nanoparticles for potential wound dressing application, *Applied Surface Science* 369 (2016) 492-500.

- [36] N. Cai, C. Han, X. Luo, S. Liu, F. Yu, Rapidly and Effectively Improving the Mechanical Properties of Polyelectrolyte Complex Nanofibers through Microwave Treatment Advanced Engineering Materials 19(1) (2017) 1600483.
- [37] S. Ahmed, S. Ikram, Chitosan Based Scaffolds and Their Applications in Wound Healing, Achievements in the Life Sciences 10(1) (2016) 27-37.
- [38] Y. Jin, D. Yang, Y. Zhou, G. Ma, J. Nie, Photocrosslinked electrospun chitosan-based biocompatible nanofibers, Journal of Applied Polymer Science 109(5) (2008) 3337-3343.
- [39] E. Salehi, P. Daraei, A. Arabi Shamsabadi, A review on chitosan-based adsorptive membranes, Carbohydrate Polymers 152 (2016) 419-432.
- [40] M. Rizwan, R. Yahya, A. Hassan, M. Yar, R. Anita Omar, P. Azari, A. Danial Azzahari, V. Selvanathan, A. Rageh Al-Maleki, G. Venkatraman, Synthesis of a novel organosoluble, biocompatible, and antibacterial chitosan derivative for biomedical applications, Journal of Applied Polymer Science 135(9) (2018) 45905.
- [41] M. Rizwan, R. Yahya, A. Hassan, M. Yar, A.A.A. Halim, A.R. Al-Maleki, L. Shahzadi, W. Zubairi, Novel chitosan derivative based composite scaffolds with enhanced angiogenesis; potential candidates for healing chronic non-healing wounds, Journal of Materials Science: Materials in Medicine 30(6) (2019) 72.
- [42] K.P. Koutroumanis, R.G. Holdich, S. Georgiadou, Synthesis and micellization of a pH-sensitive diblock copolymer for drug delivery, Int. J. Pharm. 455(1–2) (2013) 5-13.
- [43] J.T. Schantz, T.C. Lim, C. Ning, S.H. Teoh, K.C. Tan, S.C. Wang, D.W. Hutmacher, Cranioplasty after trephination using a novel biodegradable burr hole cover: technical case report, Operative Neurosurgery 58(suppl_1) (2006) ONS-E176.
- [44] M.D. Dhanaraju, D. Gopinath, M.R. Ahmed, R. Jayakumar, C. Vamsadhara, Characterization of polymeric poly(epsilon-caprolactone) injectable implant delivery system for the controlled delivery of contraceptive steroids, J Biomed Mater Res A 76(1) (2006) 63-72.
- [45] L. Du, H. Xu, Y. Zhang, F. Zou, Electrospinning of polycaprolactone nanofibers with DMF additive: The effect of solution properties on jet perturbation and fiber morphologies, Fibers and Polymers 17(5) (2016) 751-759.
- [46] V. Pillay, C. Dott, Y.E. Choonara, C. Tyagi, L. Tomar, P. Kumar, L.C. du Toit, V.M. Ndesendo, A review of the effect of processing variables on the fabrication of electrospun nanofibers for drug delivery applications, Journal of Nanomaterials 2013 (2013) 22.
- [47] R. Braga, F. Rivera, J. Moreira, A Practical Guide to Biospeckle Laser Analysis: Theory and Software, Lavras: Editora UFLA (2016).